THE JOURNAL OF BIOLOGICAL CHEMISTRY
Vol. 279, No. 30, Issue of July 23, pp. 30973–30982, 2004

*Printed in U.S.A.*

# Molecular Characterization of Two Novel Antibacterial Peptides Inducible upon Bacterial Challenge in an Annelid, the Leech *Theromyzon tessulatum**

Received for publication, November 6, 2003, and in revised form, April 9, 2004
Published, JBC Papers in Press, April 21, 2004, DOI 10.1074/jbc.M312156200

**Aurélie Tasiemski‡, Franck Vandenbulcke‡, Guillaume Mitta‡§, Jérôme Lemoine¶, Christophe Lefebvre‡, Pierre-Eric Sautière‡, and Michel Salzet‡‖**

*From the ‡Centre National de la Recherche Scientifique, Laboratoire de Neuroimmunologie UMR 8017, SN3, Université des Sciences et Technologies de Lille, 59655 Villeneuve d'Ascq, France and the ¶Centre National de la Recherche Scientifique, Laboratoire de Glycobiologie Structurale et Fonctionnelle UMR 8576, C9, Université des Sciences et Technologies de Lille, 59655 Villeneuve d'Ascq, France*

**Two novel antimicrobial peptides named theromacin and theromyzin were isolated and characterized from the coelomic liquid of the leech *Theromyzon tessulatum*. Theromacin is a 75-amino acid cationic peptide containing 10 cysteine residues arranged in a disulfide array showing no similarities with other known antimicrobial peptides. Theromyzin is an 86-amino acid linear peptide and constitutes the first anionic antimicrobial peptide observed in invertebrates. Both peptides exhibit activity directed against Gram-positive bacteria. Theromacin and theromyzin cDNAs code precursor molecules containing a putative signal sequence directly followed by the mature peptide. The enhancement of theromacin and theromyzin mRNA levels has been observed after blood meal ingestion and upon bacterial challenge. *In situ* hybridization revealed that both genes are expressed in large fat cells in contact with coelomic cavities. Gene products were immunodetected in large fat cells, in intestinal epithelia, and at the epidermis level. In addition, a rapid release of the peptides into the coelomic liquid was observed after bacterial challenge. The presence of antimicrobial peptide genes in leeches and their expression in a specific tissue functionally resembling the insect fat body provide evidence for the first time of an antibacterial response in a lophotrochozoan comparable to that of holometabola insects.**

All of the multicellular organisms including plants, invertebrates, and vertebrates have developed an immediate response to defend themselves against infectious microorganisms (1, 2). Recent studies on the components of the innate immune system have demonstrated the contribution of antimicrobial peptides to the host defense. Antibiotic peptides are small molecules. Based on their structural features, three classes were defined: 1) linear $\alpha$-helical peptides without cysteines of which the prototype of this family is the cecropin; 2) open-ended cyclic cysteine-rich peptides among which defensins are the most widespread; and 3) linear peptides containing a high proportion of one or two amino acids like indolicidin, for example (3). Despite great diversity in the primary structure, the majority of antimicrobial peptides documented are characterized by a preponderance of cationic and hydrophobic amino acids. This amphipathic structure allows them to interact with bacterial membrane. Brogden *et al.* (4) have determined in ovine that a novel class of peptides with anionic properties also has antimicrobial properties (4). In marked contrast to cationic antimicrobial peptides, no anionic antibacterial molecules have been described hitherto in invertebrates.

Antimicrobial peptides appear to be essential anti-infectious factors that have been conserved during evolution. Meanwhile, their implications in immune processes are different according to species, cells, and tissues (5). The involvement of antimicrobial peptides in natural resistance to infection is sustained by their strategic location in phagocytes, in body fluids, and at the epithelial level, *i.e.* at interfaces between the organisms and its environment. This action is strengthened by the rapid induction of such antibacterial peptide genes in bacteria-challenged plants or animals. *Drosophila melanogaster*, which is subjected to septic injury, massively induces and synthesizes a battery of potent antibiotic molecules from fat body, a functional equivalent of the mammalian liver (6). The active peptides then are released into the hemolymph where they exert their antifungal and/or antibacterial activities. Adding to their systemic response, antibiotic molecules of the fruitfly are produced by cells of most of the barrier epithelia such as tracheal epithelium, gut lining, or salivary glands where they provide a local first defense against microorganisms (7, 8).

In worms, even if antimicrobial activities have been detected in the body fluids of several species, antimicrobial peptides have been characterized fully in nematodes and annelids only. A 71-amino acid peptide named ASABF[1] (for *Ascaris suum* antibacterial factor) possessing structural and functional similarities to the insect/arthropod defensins has been characterized in the parasitic nematode as *A. suum* (9). Recently, Pillai *et al.* (10) show an enhancement of the ASABF transcript in the

* This work was supported by the Agence Nationale de Valorisation de la Recherche, the CNRS, the Ministére de l'Education Nationale de la Recherche et de la Technologie, the Fonds Europeens de Developpement Régional, the Genopole, and the Conseil Régional Nord-Pas de Calais. The costs of publication of this article were defrayed in part by the payment of page charges. This article must therefore be hereby marked "*advertisement*" in accordance with 18 U.S.C. Section 1734 solely to indicate this fact.

*The nucleotide sequence(s) reported in this paper has been submitted to the GenBank™/EBI Data Bank with accession number(s) AY434032 and AY434033.*

§ Present address: Centre de Biologie et d'Ecologie Tropicale et Méditerranéenne, Université de Perpignan, Ave. de Villeneuve, 66860 Perpignan Cedex, France.

‖ To whom correspondence should be addressed. Tel.: 33-3-20-43-68-39; Fax: 33-3-20-43-40-54; E-mail: michel.salzet@univ-lille1.fr.

[1] The abbreviations used are: ASABF, *Ascaris suum* antibacterial factor; ACN, acetonitrile; RP-HPLC, reversed-phase high pressure liquid chromatography; MALDI-TOF, matrix-assisted laser desorption ionization time-of-flight; MS, mass spectrometry; MIC, minimal inhibitory concentration; ISH, *in situ* hybridization; LFC, large fat cells.

body wall upon bacterial challenge. ASABF presents a significant sequence identity with peptides deduced from a cDNA sequence (yk150c7) and from a putative gene (T22H6.5) of the free-living nematode *Caenorhabditis elegans*. Although no variation of the *C. elegans* ASABF gene expression was detected using high density cDNA microarray, Mallo *et al.* (11) demonstrate that Gram-negative bacteria infection of this worm provokes a marked up-regulation of genes encoding lysozyme and lectins that are known to be involved in the immune responses of other species. These authors (11) also establish that certain infection-inducible genes are under the control of the DBL-transforming growth factor-$\beta$ pathway. The existence of an inducible immune system in both nematodes and insects is consistent with the new molecule-based phylogeny, which considers that protostomes can be divided into two large groups: 1) ecdysozoans comprising nematodes, arthropods, and other phyla that have emerged and 2) lophotrochozoans regrouping annelids, flat worms, and mollusks (12). In lophotrochozoans, no inducible antimicrobial peptides have been described so far in the animals studied. The gene encoding lumbricin I, a proline-rich antibacterial peptide from the earthworm *Lumbricus rubellus*, is expressed constitutively (13). The constitutive expression also has been reported in the mussel *Mytilus galloprovincialis* in which antibiotic peptides stored in hemocyte granules are released after bacterial challenge (14).

In this study, we report the primary and secondary structures of two new antibacterial peptides, theromacin and theromyzin, isolated from the body fluid of an annelid, the leech *Theromyzon tessulatum*. Interestingly, both molecules do not present significant similarities with other known molecules. Theromacin is a novel cysteine-rich antimicrobial peptide, and theromyzin constitutes a new anionic antibiotic peptide. In an experimental model of infection, we obtained evidence for an enhancement of transcription levels of both genes in specific tissues that could be assimilated to the fat body of *D. melanogaster*. We have found that peptides are released massively into hemolymph where they might exert their antimicrobial activity by a systemic action. These data, reminiscent of the *Drosophila* antimicrobial defense, are the first reports of antimicrobial peptide induction by a specific tissue in a lophotrochozoan.

## EXPERIMENTAL PROCEDURES

### *Animals*

*T. tessulatum* rhynchobdellid leech is an ectoparasite of aquatic birds. Its life cycle is subdivided in stages defined by taking as indicators three blood meals (stage 0, from hatching until the first blood meal; stages 1, 2, and 3, respectively, after the first, second, and third blood meals). The stage 3 corresponds to the gametogenesis phase.

### *Theromacin and Theromyzin Purification Procedure*

Stage 3 animals were pricked individually with saline solution or with 10 $\mu$l of a solution containing $10^9$ killed *Escherichia coli* (D31). Coelomic fluid and mucus covering the animals were collected with a tuberculin syringe at $t = 0$, 3, and 24 h after challenge. Liquids were centrifuged immediately at 800 $\times$ *g* for 15 min at 4 °C, and supernatants were diluted (1:1 v/v) in pure water (Beckman) containing 0.1% of trifluoroacetic acid. The pH value was brought to 3.9 with 1 M HCl. Centrifugation (10,000 $\times$ *g*, 20 min, at 4 °C) then was used to clarify the supernatants, which were loaded onto Sep-Pak C18 Vac cartridges (Waters) according to Bulet *et al.* (15). Elution steps were performed with 5 and 40% acetonitrile (ACN) in acidified water. The prepurified fractions then were concentrated, reconstituted in pure water, and tested for antimicrobial activity as described below. Only the 40% ACN eluted fractions were active and submitted to purification by reversed-phase high pressure liquid chromatography (RP-HPLC). All of the following HPLC steps were carried out on a Beckman™ Gold HPLC system.

*Step 1*—Aliquots of the 40% Sep-Pak fractions were subjected to RP-HPLC on a Sephasyl C18 column (250 $\times$ 4.1 mm, model 218TP54, Vydac). Elution was performed with a linear gradient of 2–52% ACN in acidified water over 90 min at a flow rate of 1 ml/min. The fractions corresponding to absorbance peaks were collected in polypropylene tubes, dried, reconstituted in water, and tested for antimicrobial activity.

*Step 2*—The active fractions were loaded further onto a C18 column (250 $\times$ 2.1 mm, model 218TP52, Vydac) with a gradient consisting of 2–25% ACN in acidified water for 10 min and 25–35% ACN for 40 min at a flow rate of 0.2 ml/min. The fractions were collected and treated as above.

*Step 3*—One additional step was performed on a Narrowbore C18 reversed-phase column (150 $\times$ 2 mm, Waters) at a flow rate of 0.2 ml/min using the ACN gradient described in Step 2.

The purity assessment and the molecular weight determination of theromacin and theromyzin were carried out by mass spectrometry in an electrospray-positive ion mode using Quattro II triple quadrupole (Micromass) and by the matrix-assisted laser desorption ionization time-of-flight (MALDI-TOF) instrument (DE STR PRO, Applied Biosystems). Amino acids analysis of the purified peptides was performed by automated Edman degradation on a pulse liquid automatic peptide sequenator (Procise, Applied Biosystems).

### *Secondary Structure Determination of Theromacin*

MALDI-TOF MS analyses were used to determine the mass of the reduced-alkylated theromacin and the mass of the fragments derived from protease digestions.

*Reduction and Alkylation*—50 pmol of purified peptide were dissolved in 100 $\mu$l of 0.2 M amino bicarbonate buffer, pH 8, containing 0.05 M dithiothreitol and 6 M guanidine hydrochloride. The sample was flushed with argon and incubated at 70 °C for 30 min. 50 $\mu$l of 6 M acrylamide was added, and the sample was flushed with argon again and incubated at 4 °C for 1 h.

*C-Lysyl Endopeptidase Digestion*—10 pmol of purified theromacin were dissolved in 10 $\mu$l of 25 mM Tris-HCl buffer, pH 8.5, containing 1 mM EDTA. 0.05 $\mu$g of lysyl endopeptidase (Roche Applied Science) was added. The digestion was carried out overnight at room temperature.

*C-Glutamyl Endopeptidase Digestion*—10 pmol of purified peptide were dissolved in 10 $\mu$l of 25 mM ammonium carbonate buffer, pH 8. 0.05 $\mu$g of glutamyl endopeptidase (Roche Applied Science) was added. This enzyme cleaves peptide bonds C-terminally at glutamic acid and with a lower rate at the aspartic residue.

MALDI-TOF MS analyses were used to measure the mass shifts of theromacin, resulting from the reduction and alkylation steps as well as the mass of the peptide fragments derived from protease digestions. The samples were dissolved in 0.5% formic acid containing methanol/water (1:1) at a concentration of 1 pmol/$\mu$l. 1 $\mu$l of the sample solution was mixed directly onto the target with 1 $\mu$l of the 2,5-dihydroxybenzoic acid matrix solution (12 mg/ml prepared in methanol/water, 7:3).

### *Bioassays*

*Microorganisms*—The bacteria *E. coli* D31, *Micrococcus luteus* IFO12708, and the filamentous fungus *Fusarium oxysporum* were used for the antimicrobial assays.

*Antimicrobial Tests*—After each purification step, antibacterial activity was monitored by a liquid growth inhibition assay as described by Bulet *et al.* (15). The minimal inhibitory concentration (MIC) and the minimal bactericidal concentration were determined according to the method of R. E. Hancock (www.interchg.ubc.ca/bobh/methods.html). Antifungal activity was monitored as described by Fehlbaum *et al.* (17) by a liquid growth inhibition assay. The bactericidal test was performed as described previously (18).

### *cDNA Cloning*

cDNA for theromacin and cDNA for theromyzin were cloned using two-step PCR amplification.

*Step 1: Reverse Transcriptase-PCR*—Total RNA from whole leech was extracted using TRIzol (Invitrogen). RNA (3 $\mu$g) was transcribed into single-stranded cDNA using the oligo(dT)$_{18}$-adaptator primer 5′-CGAGTCGACATCGATCG(T)$_{18}$-3′ (Kit Superscript™, Invitrogen, the protocol of the manufacturer). One-fourth of the reaction was amplified by PCR using the oligo(dT) primer and the degenerate sense oligonucleotide pool whose sequence was deduced from Gly$^1$-Ser$^7$ with a designated 5′-flanking sequence, 5′-GGGAATTCGG(A/T/G/C)TG(C/T)TT-(C/T)GA(A/G)GA(C/T)TGGAG-3′, for theromacin cDNA cloning and from Asp$^1$-Gly$^7$ with a designated 5′-flanking sequence, 5′-GGGAATTC-GA(C/T)CA(C/T)CA(C/T)CA(C/T)GA(C/T)CA(C/T)GG-3′, for theromyzin cDNA cloning. PCR was performed for 25 cycles using one unit of *Taq* polymerase (Appligene Quantum) in 1.5 mM $MgCl_2$. The cycling parameters were as follows: 94 °C for 1 min; 50 °C for 1 min; and 72 °C for 1 min.

*Step 2: Rapid Amplification of 5′-cDNA End*—Reverse transcription was performed using antisense oligonucleotides 5′-TTGCAGTTCTGTAGCGTTTATGC-3′ and 5′-ATCAACTGGAGTCTTATCGGCGTA-3′ deduced, respectively, from the theromacin and theromyzin cDNA sequences obtained previously. After first strand cDNA synthesis and the addition of a poly(dA) tail at its 3′ end using a terminal transferase (Invitrogen, the protocol of the manufacturer), PCR was performed with an oligo(dT) anchor primer and the internal antisense primers deduced from the cDNA obtained in Step 1 (5′-CATTCTCCCCTATCAGCTTTG-3′ for theromacin and 5′-CAGCGTTAATTCTTCGTGTTC-3′ for theromyzin). PCR parameters were identical to those described in step 1. All of the PCR products were subcloned into pGEM-T Easy vector (Promega), and several different cDNA clones were sequenced.

### *Gene Expression Site*

*In Situ Hybridization (ISH)*—Leeches were fixed overnight in a solution containing 13% formalin, 39% ethanol, and 0.65% ammonium hydroxide, pH 6.4. After dehydration, animals were embedded in paraplast and 7-$\mu$m sections were cut, mounted on poly-L-lysine-coated slides, and stored at 4 °C until use.

The plasmids containing the coding region of theromacin and theromyzin probes were used as templates for the synthesis of the probes. Digoxigenin-UTP-labeled and [$^{35}$S]UTP-labeled antisense and sense riboprobes were generated from linearized cDNA plasmids by *in vitro* transcription using an RNA-labeling kit (Roche Applied Science). Digoxigenin-labeled riboprobes (40–100 ng/slide) and $^{35}$S-labeled riboprobes (100 ng or $1 \times 10^6$ cpm/slide) were hybridized as described previously (19). The slides were observed under a Zeiss™ Axioskop microscope.

The control consisted in replacing antisense riboprobe with the sense riboprobe. RNase control sections were obtained by adding a preincubation step with 10 $\mu$g/ml RNase A prior to hybridization.

### *Gene Expression Analysis*

*Northern Blot*—Leeches were homogenized in TRIzol using a Polytron. Total RNA was extracted according to the manufacturer's protocol (Invitrogen). 10 $\mu$g of total RNAs and size markers were separated on a 1% agarose gel electrophoresis containing 0.02 M sodium phosphate buffer, pH 7.2, and 8.5% formaldehyde and transferred to Hybond N membrane (Amersham Biosciences). Theromacin and theromyzin probes were synthesized from 332- and 405-pb fragments, respectively, amplified in the first PCR (see above). An 18 S subunit probe was also performed as control. A sense oligonucleotide, 5′-GCGGGAACGAGCGCGCGTTTATTAGAT-3′, and an antisense oligonucleotide, 5′-TGGCACCAGACTTGCCCTCCAATT-3′, were designed from the ribosomal RNA 18 S subunit of *T. tessulatum* (GenBank™ accession number AFO99942) and used in PCR experiments before being subcloned into pGEM-T Easy vector. The plasmids containing theromacin cDNA or 18 S cDNA were digested with EcoRI, and inserts were purified from 1% agarose gel using the Wizard PCR-prep DNA purification system (Promega). 25 ng of each fragments then were $^{32}$P-labeled by random priming using the Ready-to-Go DNA-labeling kit (Amersham Biosciences). Hybridization and detection were performed as described previously.

*In Situ Hybridization*—Quantification of the radiolabeling at the cellular level was performed using an Axiophot Zeiss microscope and a Biocom quantification system as established previously (20).

### *Immunohistochemical Procedures*

*Antibodies*—The chemically synthesized regions of theromacin ($Gln^{49}$-$Arg^{63}$) and theromyzin ($Lys^{26}$-$Val^{41}$) were used for the immunization procedure of rabbits and mice, respectively, according to the protocol of Agrobio.

Paraffin sections were re-hydrated and treated as follows: 1) 10 min at 20 °C in 0.15 M NaCl, 0.1 M Tris-HCl, pH 7.4, buffer (Tris-buffered saline); 2) Tris-buffered saline containing 1% bovine serum albumin, 1% normal goat serum (NGS), and 0.1% Triton X-100 for 30 min at room temperature; 3) incubation with anti-theromacin (3 $\mu$g/ml) or anti-theromyzin (3 $\mu$g/ml) IgG diluted in Tris-buffered saline containing 1% bovine serum albumin and 1% NGS overnight at room temperature; 4) $3 \times 10$ min in Tris-buffered saline; 5) 1-nm colloidal gold-labeled goat anti-rabbit or anti-mouse IgG (Amersham Biosciences) diluted 1:100 in the incubation buffer for 3 h at room temperature; 6) $3 \times 10$ min in Tris-buffered saline; 7) equilibrated $2 \times 5$ min in 0.2 M citrate buffer, pH 7.4; 8) silver amplification performed with the IntensSE kit according to the manufacturer's instructions (Amersham Biosciences) for 12 min at 20 °C; and 9) $2 \times 2$ min in distilled water. Paraffin sections then were mounted in XAM (Merck) and observed using a Zeiss Axioskop light microscope.

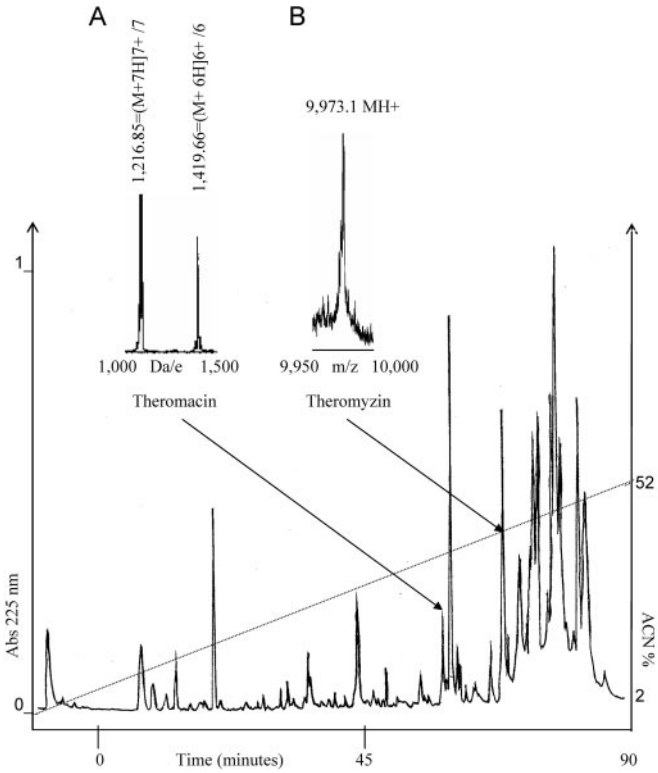


FIG. 1. **Reversed-phase HPLC of acidic extract obtained from coelomic fluid of leech.** After prepurification by solid phase extraction, the 40% ACN-eluted material was loaded onto a C18 column ($250 \times 4$ mm). Each individually collected peak was tested for its antimicrobial activity by liquid growth inhibition assays. Two fractions containing theromacin and theromyzin that were eluted at 33% ACN and at 38% ACN, respectively, were found to be active against *M. luteus*. These fractions were purified further by two additional RP-HPLC purification steps. The exact mass of purified peptides was determined by electrospray ionization MS and by MALDI-TOF MS, respectively. *A*, for theromacin mass calculation, quadrupole was scanned over 300–1700 Da. Two unequivocal pseudomolecular ions ($[M+6H]^{6+}/6$ = 1,419.66 and $[M+7H]^{7+}/7$ = 1,216.85) were observed that correspond to the protonated species whose molecular mass was 8,517.98 Da. *B*, an analysis of theromyzin by MALDI-TOF MS shows a *m/z* value of 9,973.1 MH+.

For light microscopy on 1-$\mu$m thick semi-thin sections, a post-embedding immunogold procedure was used. Tissues were fixed for 2 h at 4 °C in a mixture containing 4% paraformaldehyde, 0.1% glutaraldehyde, and 0.2% picric acid in 0.1 M phosphate buffer, pH 7.4. Tissues were post-fixed in 1% $OsO_4$ for 3–5 min and dehydrated in graded alcohol before embedding in LR-White (TAAB Laboratories). Theromacin and theromyzin immunostainings were performed using a gold-tagged secondary antibody and silver amplification as described above. Controls were incubations of immune serum preadsorbed by synthetic peptides.

### *Variation of Plasmatic Amount*

Aliquots of 40% ACN Sep-Pak and $\beta$-lactoglobulin (Applied Biosystems) at different concentrations (250, 375, and 500 pmol) were subjected to RP-HPLC on a C18 column ($250 \times 4.1$ mm, model 218TP54, Vydac). Elution was performed as described above. The area of peak corresponding to theromacin or theromyzin was calculated, and the amount of peptide was evaluated by comparing the values with the $\beta$-lactoglobulin standard. The amount obtained divided by the volume of hemolymph collected initially allowed us to estimate the concentration of theromacin in the coelomic fluid of the leech.

## RESULTS

*Biochemical and Molecular Characterization of Theromacin and Theromyzin*—Theromacin and theromyzin were isolated from leech body fluid in acidic conditions (Fig. 1). A 30-residue N-terminal sequence of the purified molecules then was obtained by automatic Edman degradation. In parallel, electro-

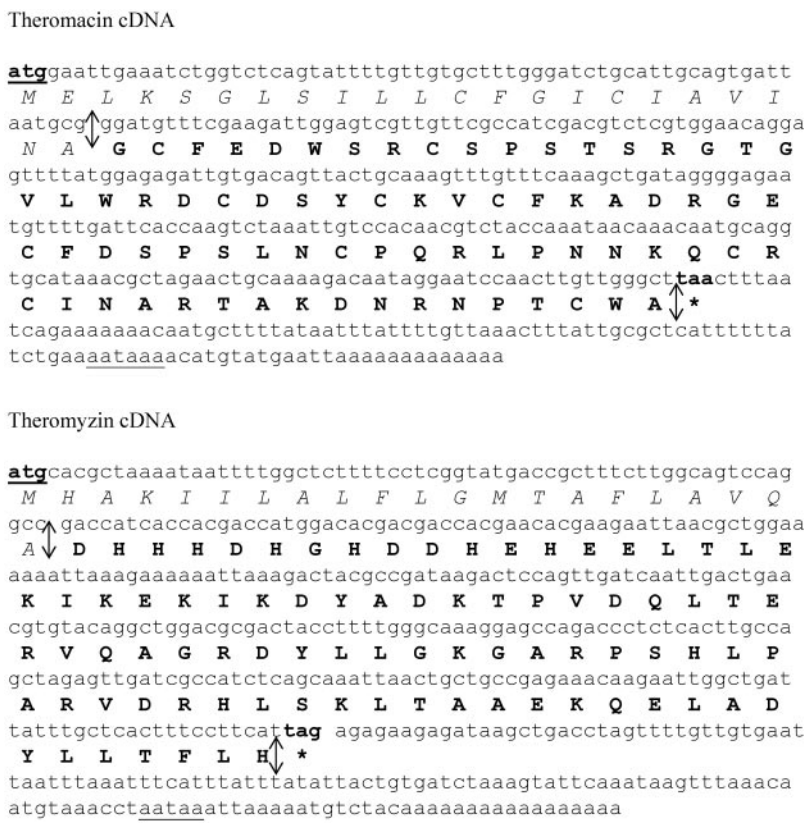


FIG. 2. **Nucleotide sequences of theromacin and theromyzin cDNAs.** Complete sequences of cDNAs were obtained by reverse transcription-PCR using degenerated oligonucleotide primers deduced from the biochemical sequence. Deduced amino acid sequences of the open reading frame are shown under the nucleotide sequence. The polyadenylation signal is *underlined*. The *double-headed arrows* indicate the limits of the mature peptide.

spray and MALDI-TOF mass spectrometry analysis revealed a deduced molecular mass of 8,517.98 Da for theromacin and 9,973.1 Da for theromyzin, illustrating that the sequences obtained by Edman degradation were incomplete (Fig. 1).

To fully determine the amino acid sequences of the peptides and to obtain information on the precursors, cDNA cloning was carried out using a two-step PCR-based approach (see "Experimental Procedures" and Fig. 2). Amino acid sequences deduced from the cDNAs allowed us to conclude that theromacin is a cationic 75-amino acid peptide (calculated pI of 8.6) and that theromyzin is an anionic 86-amino acid peptide (calculated pI of 6.03). Data bank analysis (BLAST program in Swiss-Prot) revealed no obvious sequence similarities of these peptides with other known peptides or proteins. Moreover, it appeared that the mass value corresponding to the theromacin sequence deduced from the cDNA was 10 Da in excess of the biochemically calculated mass of the native peptide (8,527.81 *versus* 8,517.98 ± 0.72). The difference in mass was attributable to the arrangement of the 10 cysteine residues contained in the sequence in five disulfide intramolecular bridges.

In contrast with theromacin, the calculated mass of theromyzin was in perfect agreement with the measured mass, demonstrating that theromyzin is a peptide devoid of post-translational modifications.

Precursor sequences also were deduced from the cDNA sequences (Fig. 2). The Signal PVI software analysis revealed that 1) theromacin and theromyzin are flanked at the N terminus by a putative hydrophobic signal peptide, $Met^{1}$-$Ala^{22}$, and $Met^{1}$-$Ala^{21}$, respectively, and that 2) the cleavage site for signal peptidase is most probably located after the $Ala^{22}$ preceding the $Gly^{23}$ for theromacin and after the $Ala^{21}$ preceding the $Asp^{22}$ for theromyzin. This leads to the notion that mature peptides may be generated through conventional processing mechanisms and can be secreted to the extracellular medium.

*Determination of the Disulfide Array of Theromacin*—To decipher the pattern of the cysteine residues engaged in disulfide bridges, the molecular mass of theromacin was subjected first to alkylation with acrylamide and then measured by MALDI-TOF mass spectrometry. The mass spectrum revealed that reducing the protein prior to the alkylation step lead to a mass shift of 710.37 Da, consistent with the incorporation of 10 acrylamide molecules, whereas alkylation alone did not lead to a mass shift (data not shown). This result demonstrates that the 10 cysteine residues of theromacin are engaged in five disulfide bridges. From the analysis of the primary structure of the antibacterial peptide showing that theromacin did not harbor a cysteine motif described in other known antimicrobial peptides, the determination of the disulfide array was visualized by protease digestion of the native peptide (Fig 3*A*).

The peptidic fragments resulting from the lysyl endopeptidase digest were analyzed by MALDI-TOF MS. As illustrated in Fig. 3, the pseudomolecular ion $[M+H^+]$ at *m/z* 1,569.65 was in perfect agreement with the connection of the fragment $Val^{30}$-$Lys^{33}$ (calculated $[M+H^+]$ ion at *m/z* 496.25) to fragment $Asp^{67}$-$Ala^{75}$ (calculated $[M+H^+]$ ion at *m/z* 1,076.45 MH+) through one intramolecular bond, $Cys^{32}$(5)-$Cys^{73}$(10) (downer numbering relative to the residue number in the theromacin sequence). The pseudomolecular ion $[M+H^+]$ at *m/z* 1,261.61 revealed the existence of an intramolecular bridge, $Cys^{57}$(8)-$Cys^{59}$(9), in the fragment $Gln^{56}$-$Lys^{66}$ (calculated $[M+H^+]$ ion at *m/z* 1,263.64). In the same manner, an intramolecular bridge, $Cys^{39}$(6)-$Cys^{47}$(7), in the fragment $Ala^{34}$-$Lys^{55}$ (calculated $[M+H^+]$ ion at *m/z* 2,461.7) was deduced from the species observed at *m/z* 2,459.96. A pseudomolecular ion, $[M+H^+]$, measured at *m/z* 3,297.5 evidenced that two disulfide bridges in the fragment $Gly^{1}$-$Lys^{29}$ (calculated $[M+H^+]$ ion at *m/z* 3,301.39) informed on the presence of two intramolecular disulfide bonds in this fragment but was not sufficient to localize the fourth and fifth disulfide bonds. The glutamyl endopeptidase digest then was investigated. The $[M+H^+]$ ion detected at *m/z* 2,358 corresponding to the fragment $Cys^{24}$(3)-$Asp^{35}$ connected to the fragment $Asn^{68}$-$Ala^{75}$ revealed the presence of an intramolecular

A

| Measured masses | Corresponding disulfide bridges | |
|---|---|---|
| **LysC digestion** ↓ | | |
| 1,569.65+/-0.1 MH+ | $VC_3FK$ DNRNPT$C_{10}$WA | 1 |
| 1,261.61+/-0.1 MH+ | $QC_8RC_9I$NARTAK | 2 |
| 2,459.96+/-0.1 MH+ | ADRGE$C_6$FDSPSLN$C_7$PQRLPNNK | 3 |
| 3,297.5+/-0.1 MH+ | G$C_1$FEDWSR$C_2$SPSTSRGTGVLWRD$C_3$DSY$C_4$K | |
| | Two bridges | 4/5 ? |
| **GluC digestion** ↓ | | |
| 2,358.1 +/-0.1 MH+ | $C_3$D SY$C_4$KV$C_5$FKAD NRNPT$C_{10}$WA | 4, 1 |

B

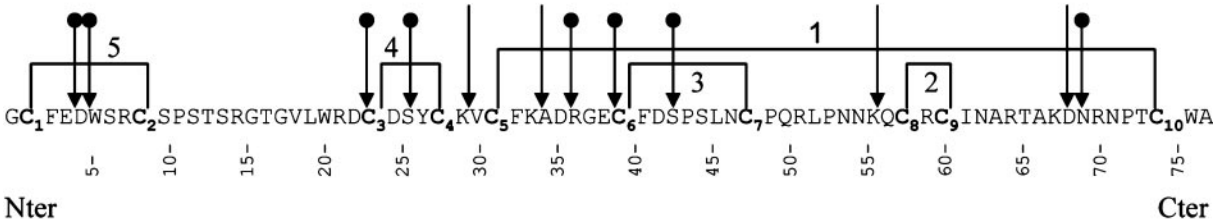


FIG. 3. **Determination of theromacin structure by analysis of the proteolysis products.** *A*, theromacin digested by a combination of endopeptidase Lys-C and endopeptidase Glu-C was concentrated, desalted, and then submitted to MALDI-TOF MS. *B*, an analysis allowed us to determine the emplacement of disulfide bridges, which are indicated by the *lines* connecting cysteine pairs.

bridge, $Cys^{24}$(3)-$Cys^{28}$(4), in the fragment $Cys^{24}$-$Asp^{35}$. By elimination, the fifth intramolecular bond links the $Cys^{2}$(1) to the $Cys^{9}$(2).

Taken together (Fig. 3*C*), these data are compatible with the following array of disulfides: $Cys^{2}$(1)-$Cys^{9}$(2); $Cys^{24}$(3)-$Cys^{28}$(4); $Cys^{31}$(5)-$Cys^{73}$(10); $Cys^{39}$(6)-$Cys^{47}$(7); and $Cys^{57}$(8)-$Cys^{59}$(9) (this array of disulfides does not present any similarities with those determined in other peptides or proteins). Theromacin is consequently a novel cysteine-rich antimicrobial peptide.

*Biological Activity of Theromacin and Theromyzin*—In liquid growth inhibition assay, the purified theromacin was active against *M. luteus* (MIC 16.5–33 nM; minimal bactericidal concentration 0.26–0.52 μM). No activity was found toward *E. coli* or *F. oxysporum* at the same concentration. When theromacin was incubated with *M. luteus* at 165 nM, a concentration 10 times higher than the MIC value, all of the bacteria were killed in <5 h (Fig. 4). Consequently, theromacin exerts a bactericidal activity. The loss of antibacterial property was noticed when theromacin was reduced, demonstrating that disulfide bridges play an important role in the biological activity of the molecule. Theromyzin was shown to be active against *M. luteus* (MIC 250–500 nM). The growth of bacteria on the plate was observed when theromyzin was tested for the minimal bactericidal concentration determination showing that the molecule possesses bacteriostatic activity against *M. luteus*.

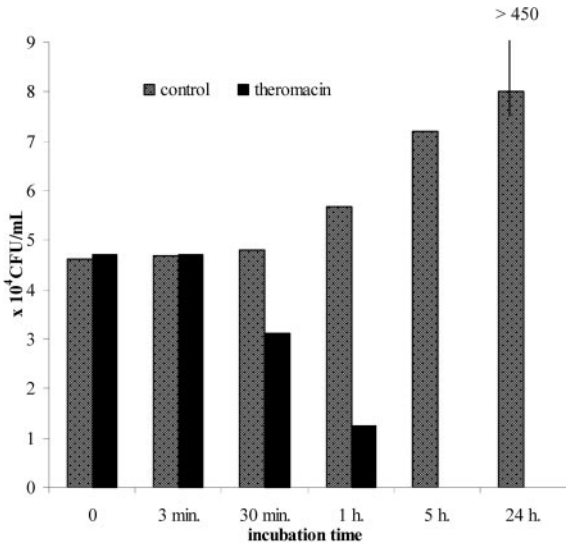


FIG. 4. **Bacteriolytic activity of 165 nM theromacin on *M. luteus*.** Water also was tested as control.

*Expression and Induction of Theromacin and Theromyzin Transcripts*—The gene expression pattern of theromacin and theromyzin during immune response was investigated by

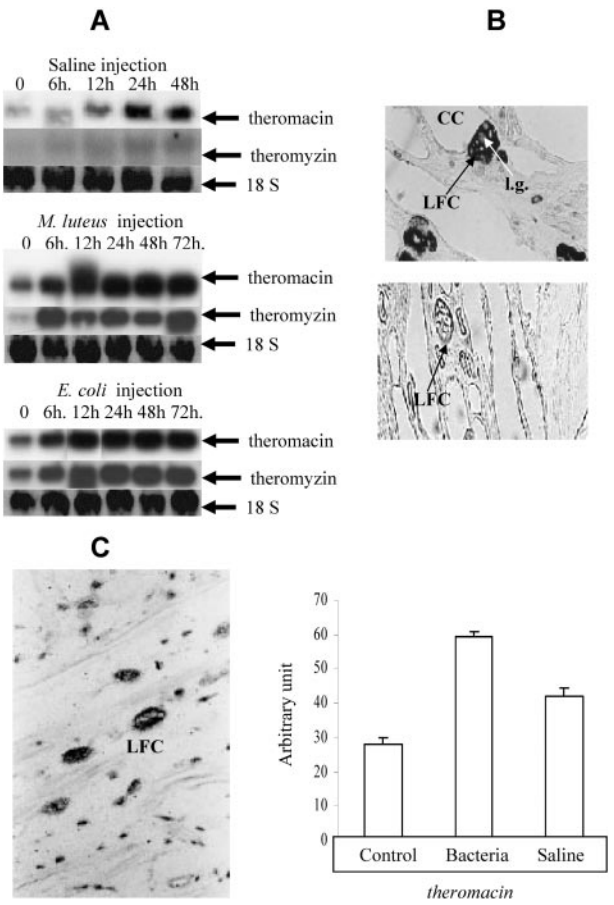


FIG. 5. **Analysis of theromacin and theromyzin gene expression in stage 3 leeches.** *A*, Northern blot analysis of RNA from stage 3 leeches extracted at different times (0, 6, 12, 24, 48, and 72h) after challenge with saline buffer, killed *E. coli*, and killed *M. luteus*. RNAs were probed successively with theromacin, theromyzin, and the 18 S ribosomal subunit cDNA. *B*, ISH with digoxygenin dUTP-labeled theromacin antisense riboprobe. The signal was detected in LFC, which are in contact with coelomic cavities (*CC*). No hybridization was noticed with the sense riboprobe, confirming the specificity of the antisense probe. *C*, ISH with radiolabeled dUTP theromacin antisense riboprobe. The signal, which appears as *dark silver deposits*, is restricted also to LFC. Individual LFC titrations of theromacin transcripts were performed using a Biocom system. The histogram shows a strong increase of the level of expression following bacterial challenge.

Northern blot. An analysis of the RNA level in stage 3 leeches was assessed first at 0, 6, 12, 24, 48, and 72 h after saline or killed bacteria (*E. coli* or *M. luteus*) injections. As illustrated in Fig. 5*A*, the theromacin and theromyzin transcripts level is enhanced rapidly (6 h) by Gram-positive bacteria, Gram-negative bacteria, or saline challenges. The expression levels were still high 3 days after infection and are stronger with a bacterial injection than with a saline injection. In contrast, no differences were observed between Gram-positive- and Gram-negative-injected leeches. Taken together, these Northern blot data indicate that treatment with bacteria induces a rapid, strong, and persistent increase of theromacin and theromyzin mRNA levels and that this enhancement does not depend on the type of septic injury. This variation of theromacin and theromyzin transcripts upon bacterial challenge also has been proven by a DNA microarray approach (21).

To corroborate these results and to better understand the physiological role of theromacin and theromyzin in stage 3 leeches, we investigated the localization of the gene expression site using ISH (Figs. 5*B* and 6*A*). Fig. 5 gives results obtained with the digoxygenin dUTP-labeled theromacin antisense probe (Fig. 5*A*) on unchallenged stage 3 leech sections. Both genes are expressed strongly and exclusively in large cells evenly distributed in whole animals. Because they contained numerous lipidic granules, we named them large fat cells (LFC). Interestingly, LFC are often in close contact with cavities containing coelomic fluid from which theromacin and theromyzin peptides were isolated. As all of these experiments were carried out with sections of non-challenged stage 3 leeches, we concluded that the RNA base-line level of stage 3 animals observed by Northern blot could be attributed to the transcripts localized in the LFC.

We then further attempted to analyze whether the inducibility evidenced by Northern blot experiments was relevant in LFC or in other tissues. The induction was monitored by injecting stage 3 leeches with bacteria or saline solution. The sections were hybridized with radiolabeled antisense riboprobes. The signal appeared under light microscopy as an accumulation of spots (Figs. 5*C* and 6*A*). The counting of the spots was performed to quantify the transcript level in the LFC (see "Experimental Procedures"). An enhancement of the theromacin (Fig. 5*C*) transcript levels was observed only in the LFC of challenged stage 3 leeches. Markedly, the level of induction in LFC was stronger with bacteria than with saline injection for both genes (41.87 *versus* 27.27 arbitrary units).

These gene expression studies were extended to stage 2 animals pricked or not (control) with saline buffer or with a mixture of killed Gram-positive and Gram-negative bacteria. ISH on sections of leeches killed 24 h post-injury was performed using radiolabeled theromacin and theromyzin riboprobes. The results are presented in Fig. 6*A*, demonstrating the detection of theromacin and theromyzin RNA in the LFC of challenged animals. The expression level was higher after bacteria injection than after saline injection (73.65 *versus* 27.27 arbitrary units for theromacin and 52.2 *versus* 18.3 arbitrary units for theromyzin). No signal was noticed in other cells or tissues.

By contrast to stage 3 animals (Fig. 5*A*), no RNA base-line level (theromacin) or very few (theromyzin) were observed in stage 2 leeches (Fig. 6*A*). The highest sensitivity of the ISH compared with Northern blot could explain why theromyzin transcripts were detected in the control by this technique only.

Thus, we hypothesized that several physiologic events that occurred during the transition stage 2/stage 3 may be inducers of theromacin and theromyzin gene expression. In support of this hypothesis, stage 2 leeches were collected 24, 48, and 72 h after the blood meal, which corresponds to the tripping factor of the transition. Total RNAs of stage 3 leeches were extracted and probed with the theromacin and theromyzin cDNA successively. The results presented in Fig. 6*B* underlined a low but progressive increase of both theromacin and theromyzin transcripts after the blood meal, confirming our hypothesis.

These results define the cells implicated in theromacin and theromyzin mRNA synthesis. We concluded that in all of the cases of induction, *i.e.* bacteria, saline injections, or transition stage 2/stage 3, the enhancement of theromacin and theromyzin transcripts was observed only in LFC. This finding suggests that the leech LFC may constitute an organ implicated in the synthesis of antimicrobial molecules comparable to the insect fat body.

*Immune Localization of Theromyzin and Theromacin Peptides and Dynamic of Their Release in the Body Fluid*—To specify the participation of theromacin and theromyzin in anti-infectious processes, immunocytochemical and plasmatic titration procedures were carried out in leeches subjected to bacterial challenge. Theromacin- and theromyzin-storing sites were investigated by immunocytochemistry on the sections of unchallenged leeches (Fig. 7). Theromacin immunoreactivity was found in LFC (Fig. 7*A*), in the intestinal epithelium (Fig. 7*B*),

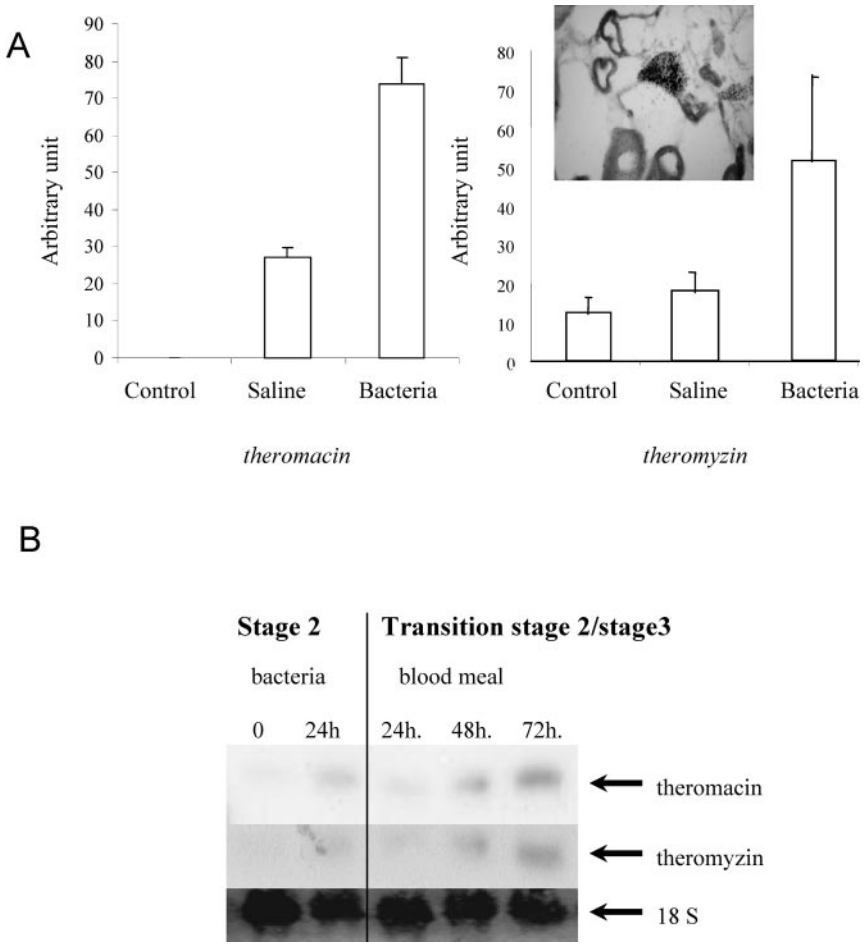


FIG. 6. *A*, ISH with radiolabeled dUTP theromyzin antisense riboprobe and quantification of the levels of expression of both antimicrobial peptides in large fat cells of stage 2 leeches 24 h after saline or bacteria injection. Control corresponds to unchallenged leeches. *B*, RNA from stage 2 leeches injected with bacteria and RNA from stage 2/stage 3 animals extracted at different times after the blood meals were probed with theromacin, theromyzin, and 18 S ribosomal subunit cDNA.

and at the epidermis level. Theromyzin immunolabeling was observed also in LFC (Fig. 7*F*). Semi-thin sections confirmed the labeling of LFC and showed a strong immunoreactivity in coelomic cavities (*CC*) in contact with the LFC when using theromacin (Fig. 7*E*) and theromyzin (Fig. 7, *F* and *G*) antisera. No immunolabeling was detected in the controls (Fig. 7, *D* and *H*), confirming the specificity of the reaction. Interestingly, these coelomic cavities contain the body fluid from which theromacin and theromyzin were isolated. These results argue in favor of an exocytosis of the antibacterial peptides from the LFC to the body fluid of the leech.

To study the effect of injury on exocytosis mechanism, a variation of theromacin and theromyzin plasmatic amounts was carried out. Leech liquid coelomic fluid was extracted at $T = 0$, 3, and 24 h after saline or bacteria injection, and variations of body fluid theromacin and theromyzin amounts were estimated by RP-HPLC. The results presented in Fig. 8 demonstrated an increase of the base-line levels of theromacin (86 nM) and theromyzin (360 nM) 3 h after bacteria or saline challenge. These rapid and massive releases were stronger in leech injected by bacteria (205.61 and 840.04 nM for theromacin and theromyzin, respectively) than by saline solution (161.3 and 600 nM for theromacin and theromyzin, respectively). It appeared that, 24 h post-injection, theromacin and theromyzin amounts returned to base-line values (68 and 280 nM, respectively). These estimations are in line with the MIC values (16.5–33 and 250–500 nM), suggesting that theromacin and theromyzin could exert their antibacterial activity into the body fluid of the animal.

We can conclude that, similar to antimicrobial peptides of *Drosophila*, theromacin and theromyzin peptides are induced principally in specialized tissue (in this case, LFC) and are released immediately into the coelomic fluid after septic injury (22).

In addition to their participation in the systemic response, theromacin and theromyzin may have a role in mucosal defense. Immunocytochemistry (Fig. 7*C*) underlined the theromacin-positive structures in the epithelia in contact with the external environment, the intestine epithelium, and epidermis. The localization at the epidermis level drove us to search for the peptides in the mucus covering the animals. This investigation also was based on the physiological observations made during the injection. Indeed, we noted a strong enhancement of mucus production by leech after bacterial challenge. After acidic extraction and RP-HPLC purification of the mucus, two peaks eluted at the same ACN percentage as theromacin and theromyzin. Sequencing by Edman degradation and MALDI-TOF MS analysis confirmed that the two molecules isolated from the mucus corresponded to theromacin and theromyzin (data not shown).

## DISCUSSION

Our study described both the isolation and characterization of two novel antibacterial peptides from the body fluid of the leech *T. tessulatum*. These are theromacin, a cationic peptide exhibiting bactericidal activities, and theromyzin, an anionic peptide with bacteriostatic properties. The peptide sequences deduced from the theromacin and theromyzin genes contain putative signal peptides, indicating that mature peptides correspond to secreted molecules. Importantly, in the context of this study, the genes encoding these peptides are up-regulated by immune challenge in a diffused tissue constituted by the LFC.

Over the last decade, several types of antimicrobial peptides containing cysteine residues have been described in multiple

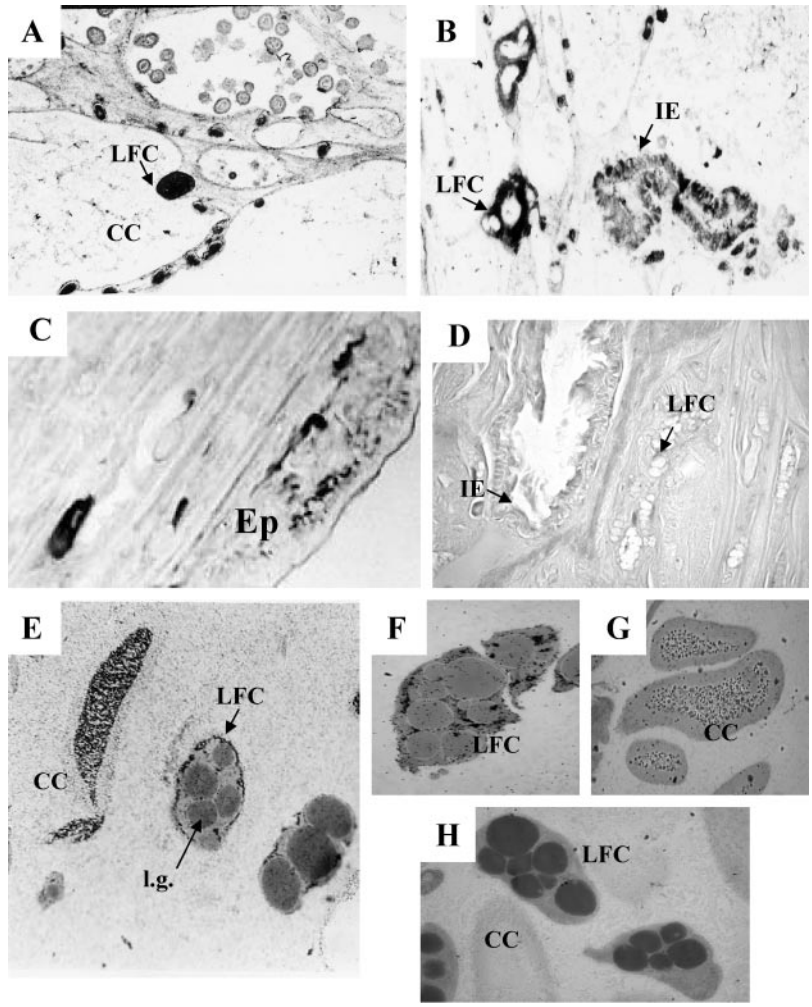


FIG. 7. **Immune localization of theromacin and theromyzin peptides in non-injected stage 3 animals.** Theromacin immunoreactivity on paraffin sections was observed in LFC (*A*), in intestinal epithelia (*IE*) (*B*), and at the epidermis level (*Ep*) (*C*). On semi-thin sections using an immunogold procedure, positive signals with both theromacin (*D* and *E*) and theromyzin antisera were detected at the periphery of the LFC (*F*) and into coelomic cavities (*CC*) (*G*). Controls (theromacin (*D*) and theromyzin (*H*)) were incubations of immune serum preadsorbed by synthetic peptides.

organisms. In invertebrates, most of them share the disulfide array of the insect/arthropod defensin: $Cys^1$-[ . . . ]-$Cys^2$-Xaa-Xaa-Xaa-$Cys^3$-[ . . . ]-Gly-Xaa-$Cys^4$-[ . . . ]-$Cys^5$-Xaa-$Cys^6$ (23). In addition to having ten cysteine residues instead of six, theromacin does not harbor this consensus sequence. Furthermore, the data bank analysis (Blast program in Swiss-Prot) showed that the peptide has no significant similarity with other known peptides. Thus, theromacin can be considered as a new cysteine-rich antimicrobial peptide. Few cysteine-rich antimicrobial peptides different from the insect/arthropod defensin have been reported in other invertebrates such as the nematode *A. suum* (9). This finding suggests that cysteine-rich antibacterial peptides could be very ancient in origin, which leads to the questions already advanced by Kato *et al.* (24). Are antibiotic cysteine-rich molecules found in plants, vertebrates, or invertebrates evolutionarily related? Do they possess a common ancestral molecule?

The majority of antimicrobial peptides including members of the cysteine-rich family possess a global positive charge, allowing their interaction with the negatively charged bacterial membrane (25). Our study shows that theromyzin, in contrast to theromacin, is an anionic molecule. This is the first report of an anionic antibacterial peptide in invertebrates. In vertebrates, antimicrobial peptides with anionic properties were evidenced in the human and in sheep lung (4). Anionic properties are anionic because of the homopolymeric regions of aspartate and require zinc as a cofactor for bactericidal activity. Histatins, a family of histidine-rich antimicrobial peptides found in human saliva, also need the presence of zinc ions for bactericidal activities (26). Circular dichroism studies showed that the antimicrobial activities of histatin 5 require a conformational change that results from the interaction of the peptide with both zinc ions and negatively charged membranes (27). The abundance of histidine residues at the N-terminal part of theromyzin could argue in favor of some common structures between the leech antibacterial peptide and histatins. Based on these data, we can hypothesize that the active part of theromyzin might be reduced to the N-terminal part enriched in histidine and aspartate residues and that theromyzin could require a cofactor for bactericidal activity.

Theromacin and theromyzin genes are expressed exclusively in LFC evenly distributed in the leech. Their transcriptional level is enhanced after bacterial challenge. These results underlined a regulation of the theromacin gene similar to that of the insect antimicrobial peptides genes. Indeed, in the fruitfly, genes encoding antibiotic peptides are induced rapidly following a septic injury and their expression is continuous over 1–3 days following a septic injury (22). Moreover, no difference in gene expression was observed after Gram-positive or Gram-negative injection, suggesting that the antibacterial response of *Theromyzon* is aspecific. This nonspecificity also has been assumed in *Drosophila* until the work of Lemaitre *et al.* (22) demonstrated that the humoral antimicrobial response of the fruitfly discriminates among various classes of microorganisms and mounts a response that is adapted to the infection. This suggests that, in a more natural mode of infection, the leech also could adapt its antimicrobial response.

In addition, it appeared that some physiological events occurring during the transition stage 2/stage 3 could also be inducers of the theromacin and theromyzin gene expression.

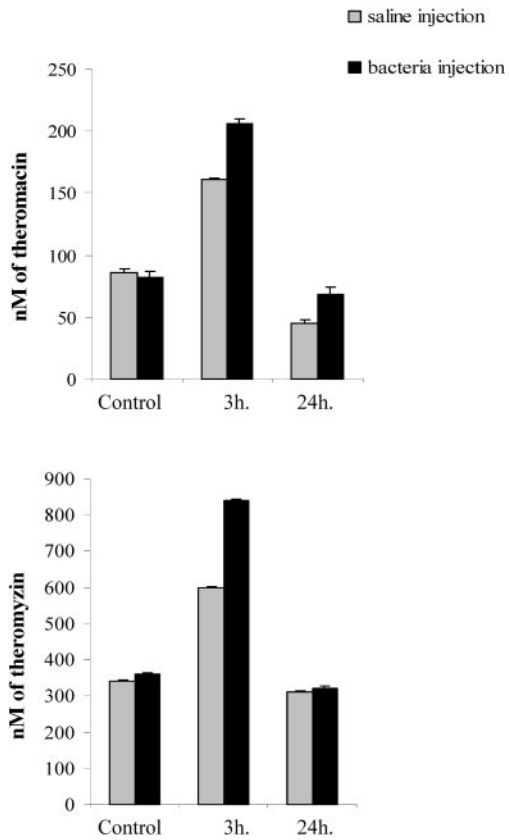


FIG. 8. **Histograms refer to variations of theromacin and theromyzin plasmatic amounts determined by RP-HPLC after saline or bacterial injection.**

Since the stage 3 leeches entered their gametogenesis phase, we hypothesized that such hormonal factors implicated in this sexual maturation may participate in the induction of theromacin and theromyzin genes. This kind of developmental induction had been reported already for the *Drosophila* diptericin gene. Meister and Richards (28) present evidence that an important increase in the response of the gene occurred during the third larval stage, leading to a maximum in late larvae and early prepupae after a septic injury.

The massive production of theromacin and theromyzin is followed immediately by a rapid release of the peptides into the coelomic fluid after septic injury. Thus, theromacin and theromyzin may play their antimicrobial activities through a systemic action. Moreover, the presence of these peptides in the intestinal epithelial cells and at the epidermis level suggests that leech antimicrobial peptides could also play a role in epithelial defense. The localization of antibiotic molecules in the gastrointestinal tract also has been reported in insects and in vertebrates where they provide a rapid local immune response against exogenous pathogens brought in during feeding (29–31). The detection of theromacin and theromyzin in leech mucous evokes the local defensive response reported in frogs in which antibacterial peptides secreted in the mucous prevent bacteria colonization and/or subsequent infection (30). In addition, because a mucous membrane covers the eggs after laying, we hypothesized a protective role of leech theromacin and theromyzin against bacteria during egg development.

The sum of these data allows us to present a scheme for the role of antimicrobial peptides in the immune system of the leech. Septic injury provokes an important production of mucous that would trap bacteria present in the external environment of the leech. The trapped bacteria then would be killed by theromacin and theromyzin present in the mucous. At the same time, injury would induce theromacin and theromyzin gene expression and the secretion of the gene products from the LFC into the body fluid of the animal. Thus, theromacin and theromyzin would exert their antimicrobial property through a systemic action. This would lead, in conjunction with the phagocytic action of coelomocytes, to the microbial killing in the body fluid.

The results presented here are in contrast with those reported for other lophotrochozoans such as the mollusk *M. galloprovincialis* and the annelid *L. rubellus* (13, 19). In these animals, antibiotic peptides are expressed constitutively and stored in hemocytes; no specific organ like the fat body is implicated. The production and secretion of active theromacin and theromyzin by a specific tissue and the rapid transcriptional up-regulation on infection evoke for the first time in a lophotrochozoan an antimicrobial response developed by holometabola insects (32, 33). Indeed, the recent data made a distinction between insects undergoing complete (holometabolas) and incomplete (heterometabolas) metamorphosis. In many studied holometabolas, *i.e.* in dipterans or in lepidopterans, antibiotic peptide genes are induced by bacterial challenge (16). In contrast, no inducible system was found in heterometabolas like the termite (isopteran). These results suggest that, in arthropods, such inducible systems of antimicrobial peptide gene could have appeared at the time of the divergence of holometabolas from heterometabola insects. The similarity between the antibacterial response of the leech and that of holometabolas also is supported by the functional resemblance between the leech LFC and the insect fat body, which possess the common capacity to produce egg yolk proteins.

*Acknowledgments*—We thank Annie Desmons for technical assistance. We are indebted to Dr. J. Vizioli for stimulating discussions, to Dr. Evelyne Bachère for the kind gift of *F. oxysporum*, to Dr J. C. Beauvillain and Dr. V. Mitchell (IFR 22, Faculté de Médecine) for access to the Cellular Imaging Center, and to Dr. J. Lesage for the precious advice in Northern blot analysis.

REFERENCES

1. Garcia-Olmedo, F., Molina, A., Alamillo, J. M., and Rodriguez-Palenzuela, P. (1998) *Biopolymers* **47,** 479–491
2. Zasloff, M. (2002) *Nature* **415,** 389–395
3. Boman, H. G. (1995) *Annu. Rev. Immunol.* **13,** 61–92
4. Brogden, K. A., De Lucca, A. J., Bland, J., and Elliott, S. (1996) *Proc. Natl. Acad. Sci. U. S. A.* **93,** 412–416
5. Salzet, M. (2001) *Trends Immunol.* **22,** 285–288
6. Hoffmann, J. A., Reichhart, J. M., and Hetru, C. (1996) *Curr. Opin. Immunol.* **8,** 8–13
7. Tzou, P., Ohresser, S., Ferrandon, D., Capovilla, M., Reichhart, J. M., Lemaitre, B., Hoffmann, J. A., and Imler, J. L. (2000) *Immunity* **13,** 737–748
8. Tzou, P., De Gregorio, E., and Lemaitre, B. (2002) *Curr. Opin. Microbiol.* **5,** 102–110
9. Kato, Y., and Komatsu, S. (1996) *J. Biol. Chem.* **271,** 30493–30498
10. Pillai, A., Ueno, S., Zhang, H., and Kato, Y. (2003) *Biochem. J.* **371,** 663–668
11. Mallo, G. V., Kurz, C. L., Couillault, C., Pujol, N., Granjeaud, S., Kohara, Y., and Ewbank, J. J. (2002) *Curr. Biol.* **12,** 1209–1214
12. Adoutte, A., Balavoine, G., Lartillot, N., Lespinet, O., Prud'homme, B., and de Rosa, R. (2000) *Proc. Natl. Acad. Sci. U. S. A.* **97,** 4453–4456
13. Cho, J. H., Park, C. B., Yoon, Y. G., and Kim, S. C. (1998) *Biochim. Biophys. Acta* **1408,** 67–76
14. Mitta, G., Vandenbulcke, F., and Roch, P. (2000) *FEBS Lett.* **486,** 185–190
15. Bulet, P., Cociancich, S., Dimarcq, J. L., Lambert, J., Reichhart, J. M., Hoffmann, D., Hetru, C., and Hoffmann, J. A. (1991) *J. Biol. Chem.* **266,** 24520–24525
16. Lamberty, M., Zachary, D., Lanot, R., Bordereau, C., Robert, A., Hoffmann, J. A., and Bulet, P. (2001) *J. Biol. Chem.* **276,** 4085–4092
17. Fehlbaum, P., Bulet, P., Chernysh, S., Briand, J. P., Roussel, J. P., Letellier, L., Hetru, C., and Hoffmann, J. A. (1996) *Proc. Natl. Acad. Sci. U. S. A.* **93,** 1221–1225
18. Mitta, G., Hubert, F., Noel, T., and Roch, P. (1999) *Eur. J. Biochem.* **265,** 71–78
19. Mitta, G., Vandenbulcke, F., Noel, T., Romestand, B., Beauvillain, J. C., Salzet, M., and Roch, P. (2000) *J. Cell Sci.* **113,** 2759–2769
20. Faure-Virelizier, C., Croix, D., Bouret, S., Prevot, V., Reig, S., Beauvillain, J. C., and Mitchell, V. (1998) *Endocrinology* **139,** 4127–4139
21. Lefebvre, C., Cocquerelle, C., Vandenbulcke, F., Hot, D., Huot, L., Lemoine, Y., and Salzet, M. (2004) *Biochem. J.*, in press
22. Lemaitre, B., Reichhart, J. M., and Hoffmann, J. A. (1997) *Proc. Natl. Acad. Sci. U. S. A.* **94,** 14614–14619

23. Bulet, P., Hetru, C., Dimarcq, J. L., and Hoffmann, D. (1999) *Dev. Comp. Immunol.* **23,** 329–344
24. Kato, Y., Aizawa, T., Hoshino, H., Kawano, K., Nitta, K., and Zhang, H. (2002) *Biochem. J.* **361,** 221–230
25. Shai, Y. (2002) *Biopolymers* **66,** 236–248
26. Brewer, D., and Lajoie, G. (2000) *Rapid Commun. Mass Spectrom.* **14,** 1736–1745
27. Brewer, D., and Lajoie, G. (2002) *Biochemistry* **41,** 5526–5536
28. Meister, M., and Richards, G. (1996) *Insect Biochem. Mol. Biol.* **26,** 155–160
29. Bevins, C. L., Martin-Porter, E., and Ganz, T. (1999) *Gut* **45,** 911–915
30. Bevins, C. L., and Zasloff, M. (1990) *Annu. Rev. Biochem.* **59,** 395–414
31. Vizioli, J., Richman, A. M., Uttenweiler-Joseph, S., Blass, C., and Bulet, P. (2001) *Insect Biochem. Mol. Biol.* **31,** 241–248
32. Engstrom, Y. (1999) *Dev. Comp. Immunol.* **23,** 345–358
33. Lamberty, M., Ades, S., Uttenweiler-Joseph, S., Brookhart, G., Bushey, D., Hoffmann, J. A., and Bulet, P. (1999) *J. Biol. Chem.* **274,** 9320–9326